DTD 5
ARTICLE IN PRESS

Available online at www.sciencedirect.com
SCIENCE DIRECT®

ELSEVIER

Physica D xxx (2004) xxx–xxx

PHYSICA D

www.elsevier.com/locate/physd

Automatic control of phase synchronization in coupled complex oscillators

Vladimir N. Belykh[a], Grigory V. Osipov[b], Nina Kuckländer[c,*], Bernd Blasius[c], Jürgen Kurths[c]

[a] *Mathematics Department, Volga State Academy, 5, Nesterova Str., 603005 Nizhny Novgorod, Russia*
[b] *Department of Radiophysics, Nizhny Novgorod University, 23, Gagarin Avenue, 603600 Nizhny Novgorod, Russia*
[c] *Institute of Physics, University Potsdam, PF 601553, D-14415 Potsdam, Germany*

Received 18 March 2004; received in revised form 29 September 2004; accepted 1 October 2004

Communicate by R. Roy

Abstract

We present an automatic control method for phase locking of regular and chaotic nonidentical oscillations, when all subsystems interact via feedback. This method is based on the well known principle of feedback control which takes place in nature and is successfully used in engineering. In contrast to unidirectional and bidirectional coupling, the approach presented here supposes the existence of a special controller, which allows to change the parameters of the controlled systems. First we discuss general principles of automatic phase synchronization (PS) for arbitrary coupled systems with a controller whose input is given by a special quadratic form of coordinates of the individual systems and its output is a result of the application of a linear differential operator. We demonstrate the effectiveness of our approach for controlled PS on several examples: (i) two coupled regular oscillators, (ii) coupled regular and chaotic oscillators, (iii) two coupled chaotic Rössler oscillators, (iv) two coupled foodweb models, (v) coupled chaotic Rössler and Lorenz oscillators, (vi) ensembles of locally coupled regular oscillators, (vii) ensembles of locally coupled chaotic oscillators, and (viii) ensembles of globally coupled chaotic oscillators.

PACS: 05.45.+b

Keywords: Phase synchronization; Feedback control; Phase locked loops

* Corresponding author. Tel.: +49 331 977 1118; fax: +49 331 977 1142.
E-mail address: nina@agnld.uni-potsdam.de (N. Kuckländer).

0167-2780/$ – see front matter © 2004 Elsevier B.V. All rights reserved.
doi:10.1016/j.physd.2004.10.008

1. Introduction

Synchronization is an important phenomenon observed in nature and science [1]. Synchronization in a dynamical system is the phenomenon of the onset of *balance* between the phases of the subsystems' state variables' oscillations, which is caused by an onset of the energy balance due to interaction. This phenomenon is called phase synchronization (PS). Especially, PS is typical for many systems in biology and neuroscience [2,3] or physics [4]. The balance of the phases of oscillations can be accompanied with a balance of the corresponding amplitudes. In this case generalized synchronization (GS) can be observed in dynamical systems and in the case of the full coincidence of synchronized variables the complete (full) synchronization sets in (for a review see, e.g. [5]). Depending on the type of coupling two main classical cases of synchronization can be distinguished: external and mutual. In the former case a freely evolving master system, acting as an external force, drives the slave system. Often, the increasing of the external force leads to locking-in, and synchronization occurs. Note that such a drive-response (or master-slave) configuration is frequently used in chaotic communication [6]. Mutual synchronization can be observed in the case of bidirectional coupling and is commonly accompanied by the hysteresis phenomenon [7].

We propose an automatic control method of phase locking of regular and chaotic nonidentical oscillations, when all subsystems interact via a feedback. This method is based on the well known principle of feedback control which takes place in nature and is successfully used in engineering. Considering the models of coupled systems in biology, neuroscience or ecology, one can see that in many of them the coupling between interacting elements is *nonlinear*, and it usually has the form of quadratic functions of the subsystem variables. Such a coupling serves as the basis of an internal self-organization mechanism leading to a balanced motion in these systems. Coupled neurons [8], phase transitions in human hand movement [9], ecological systems [10], or spinal generators of locomotion [11], are only some well known examples of balanced cooperative oscillatory motion, caused by a nonlinear coupling. In engineering, nonlinear coupling, is used, for example, in coupled lasers [12] or phase locked loops (PLL) [13].

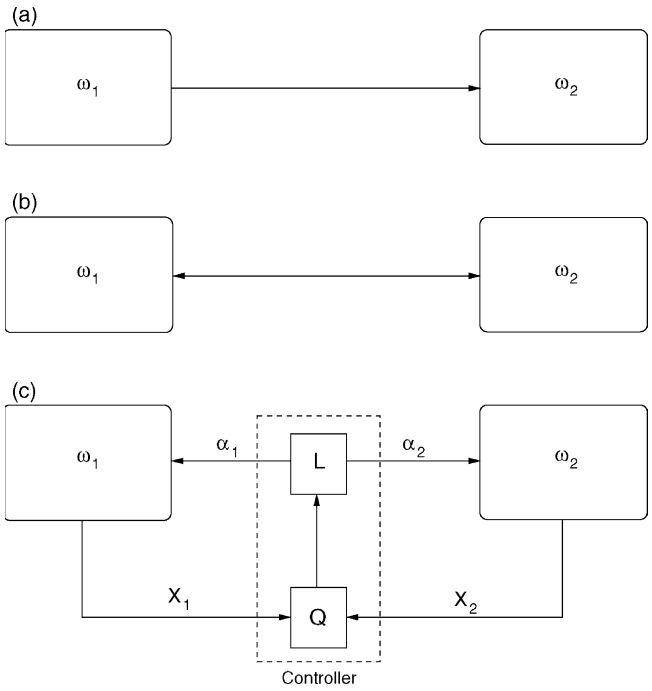

Fig. 1. Three main schemes of inter-element coupling between two oscillators having natural frequencies ω_1 and ω_2: (a) unidirectional, (b) bidirectional, and (c) coupling via a feedback loop with controller composed of quadratic form (4) and linear operator (3).

Different methods for controlling the behavior of dynamical systems have been used for chaos control [14]. An adaptation of these methods for the stabilization of a chaotic trajectory of one system to a chaotic trajectory of another *identical* system, i.e. for a *control of complete synchronization*, was presented in [15]. In [16] it was shown that the main problems of *complete* synchronization being regarded as a control problem can be solved on the basis of control theory methods. On the other hand, the problem of *phase* synchronization has not been formulated and hence considered before as a control theory problem. In contrast to the aforementioned methods, our novel approach is directed at controlling the phases via characteristic time scales (CTS) of two (or many) different interacting oscillators.

In contrast to unidirectional (Fig. 1a) and bidirectional (Fig. 1b) coupling, the approach presented here supposes the existence of a special controller, which allows to change the parameters of the controlled systems (Fig. 1c). For this purpose we extract first the mutual correlation between the CTS, then filter the obtained signal, and finally change the systems' parameters which govern the CTS.

The paper is structured as follows: first we discuss general principles of automatic phase synchronization (PS) for arbitrary coupled systems with a controller whose input is given by a special quadratic form of the coordinates of the individual systems and its output is a result of the application of a linear differential operator. Then, we demonstrate the effectiveness of our approach for controlled PS on several examples: (i) two coupled regular oscillators, (ii) coupled regular and chaotic oscillators, (iii) two coupled chaotic Rössler oscillators, (iv) two coupled foodweb models, (v) coupled chaotic Rössler and Lorenz oscillators, (vi) ensembles of locally coupled regular oscillators, (vii) ensembles of locally coupled chaotic oscillators, (viii) ensembles of globally coupled chaotic oscillators, and (ix) other forms of this control mechanism.

2. General principles of automatic synchronization

To begin with, we describe automatic phase locking for the case of two arbitrary regular or chaotic oscillators given by the system:

$$\dot{x}_{1,2} = F_{1,2}(x_{1,2}, \omega_{1,2}), \tag{1}$$

where $x_{1,2}$ and $F_{1,2}$ are n-dimensional vectors, $\omega_{1,2}$ are parameters defining the time dependence rate (in some cases, frequencies) of oscillators $x_{1,2}(t)$ [17]. Our purpose is to synchronize such two oscillators by using a feedback control of the time scales of coupled oscillators in such a way that the new characteristic time scales $\Omega_{1,2}^{-1}$ become identical. Here $\Omega_{1,2}$ are the mean observed frequencies of the controlled oscillators. In addition to the comparison of the observed frequencies of the controlled systems, we are also interested in the evolution of their phase difference, which is typically used in the study of PS. In order to synchronize the coupled subsystems, we apply a feedback control in the following form:

$$\begin{aligned} &\dot{x}_{1,2} = F_{1,2}(x_{1,2}, \omega_{1,2}(1 + \alpha_{1,2}u)), \\ &Lu = Q(x_1, x_2). \end{aligned} \tag{2}$$

Here L is a linear operator

$$L = \gamma_k \frac{\mathrm{d}^k}{\mathrm{d}t^k} + \gamma_{k-1} \frac{\mathrm{d}^{k-1}}{\mathrm{d}t^{k-1}} + \cdots + \gamma_1 \frac{\mathrm{d}}{\mathrm{d}t} + a_0 \tag{3}$$

acting as a low-pass filter, all γ_k are nonnegative constants. $Q(x_1, x_2)$ is a quadratic form

$$Q = x_1^T H x_2, \tag{4}$$

where H is a $n \times n$ matrix, which usually is taken as a diagonal matrix. $\alpha_{1,2}$ are the feedback controlling coefficients, acting on the subsystems 1 and 2, respectively and $u(t)$ is the control variable, which is added in (1) in such a way that it is able to change the characteristic time scales of the interacting subsystems.

The scheme modeled by Eqs. (2)–(4) works in the following simple manner: first, the two signals x_1 and x_2 taken from both interacting systems are fed to the *multiplier*, $Q(x_1, x_2)$, which is acting as a correlator between the variables of the interacting systems (first part Q of the "Controller" presented in Fig. 1c). The spectrum of oscillations $Q(t)$ consists of a "low" part defined by the difference $\Omega_2 - \Omega_1$ and a "high" part defined by the sum $\Omega_2 + \Omega_1$. Then, the signal $Q(t)$ is conducted through the low-pass filter (second part L of the "Controller" presented in Fig. 1c), which damps the "high" frequency part due to a specially designed transfer function. Hence, the control variable $u(t)$ becomes a slow-varying function in time, whose spectral band goes to zero. After the filtering, $u(t)$ is added to both interacting systems (2) in such a way that it may change their characteristic time scales. The main goal is that this procedure provides a balance between the new time scales, i.e. $\Omega_2 = \Omega_1$. Note, that due to the boundedness of the form $Q(x_1^*, x_2^*)$ at the attractor and due to the stability of the operator L, the control variable u is bounded too, i.e. $\|u(t)\| < K$, where $K = \text{const}$.

This principle of obtaining synchronization is effectively used in applications of PLL in a large number of radio- and telecommunication devices, radio-location [13], coupled lasers [12], etc. It also takes place in a huge variety of examples in nature, where the interaction of some *oscillatory* objects leads to their *balanced* behavior. This balanced behavior is achieved by a *nonlinear interaction* of the elements [10,18–23]. Usually this coupling has the form of a quadratic function of the interacting elements [24]. This type of coupling is able to minimize the oscillator's phase difference and therefore leads to synchronization. It is important to emphasize that this principle can be applied not only to coupled self-oscillatory systems. This will be covered in the last section.

3. Two coupled Poincaré systems

As the simplest case, we consider feedback control of PS in two coupled Poincaré systems

$$\begin{aligned}
\dot{x}_1 &= -\omega_1(1+\alpha_1 u)y_1 - \lambda(x_1^2 + y_1^2 - p^2)x_1,\\
\dot{y}_1 &= \omega_1(1+\alpha_1 u)x_1 - \lambda(x_1^2 + y_1^2 - p^2)y_1,\\
\dot{x}_2 &= -\omega_2(1+\alpha_2 u)y_2 - \lambda(x_2^2 + y_2^2 - p^2)x_2,\\
\dot{y}_2 &= \omega_2(1+\alpha_2 u)x_2 - \lambda(x_2^2 + y_2^2 - p^2)y_2,\\
\tau\dot{u} &= -\gamma u + \beta x_1 x_2.
\end{aligned} \tag{5}$$

Here, (x_i, y_i) describe the two Poincaré systems and u is the control variable. $\omega_{1,2}$ are the frequencies, p is the amplitude of oscillations and $\lambda > 0$ determines the relaxation to the limit cycle. β and γ are the parameters of the controller. The constants $\alpha_{1,2}$ determine the coupling scheme. By a simple modification of α_i it is possible to realize both bi-directional ($\alpha_i \neq 0,\ i \in \{1, 2\}$) or uni-directional coupling ($\alpha_i = 0,\ \alpha_j \neq 0$). Notice, that in this scheme the coupling strength α_i may as well take negative numbers. In (5) we have taken very simple forms for the quadratic form $Q(x_1, x_2) = \beta x_1 x_2$ and the linear operator $L = \tau \mathrm{d}/\mathrm{d}t + \gamma$. However, we note that also different, more sophisticated, functions may be used with similar results. For example, we have checked that synchronization indeed occurs with different quadratic forms such as $Q(x_1, x_2) = (x_1 - x_2)^2$ or $Q(x_1, y_2) = (x_1 - y_2)^2$.

Using polar coordinates $x_i = \rho_i \cos\phi_i$, $y_i = \rho_i \sin\phi_i$, we rewrite system (5) in the form:

$$\begin{aligned}
\dot{\rho}_{1,2} &= \lambda\rho_{1,2}(p^2 - \rho_{1,2}^2),\\
\dot{\phi}_{1,2} &= \omega_{1,2}(1+\alpha_{1,2}u),\\
\tau\dot{u} &= -\gamma u + \beta\rho_1\rho_2\cos(\phi_1)\cos(\phi_2).
\end{aligned} \tag{6}$$

The product of cosine functions in (6) can be decomposed into a slow and a rapidly oscillating term. In the limit $\omega_1 + \omega_2 > \gamma$, the low pass filter L is damping out the 'high' frequencies, which further simplifies the dynamics. Let $\omega_2 = \omega_1 + \Delta$. After relaxation of the radial equation, $\dot{\rho}_i = 0$, the amplitude of each oscillator is fixed to $\rho_i = p$. Thus, after averaging we arrive at the following simplified equations for the control variable u and the phase

difference $\theta = \phi_2 - \phi_1$:

$$\begin{aligned} \dot{\theta} &= \Delta + (\alpha_2\omega_2 - \alpha_1\omega_1)u, \\ \tau\dot{u} &= -\gamma u + \tfrac{1}{2}(\beta\, p^2)\cos\theta. \end{aligned} \tag{7}$$

Rewritten as a second order differential equation this leads to

$$\tau\ddot{\theta} + \gamma\dot{\theta} - \gamma\Delta - \tfrac{1}{2}(\beta)p^2(\alpha_2\omega_2 - \alpha_1\omega_1)\cos\theta = 0. \tag{8}$$

This pendulum-like equation for the evolution of the phase difference describes the synchronization regime of the two oscillators interacting via feedback control. The existence of this regime is defined by a stable steady state in (7) with the coordinates

$$\cos\theta^* = \frac{2\gamma}{\beta p^2}u^*, \quad u^* = \frac{\Delta}{\alpha_1\omega_1 - \alpha_2\omega_2}, \tag{9}$$

which does exist in the range

$$\frac{\beta p^2}{2\gamma} > \left|\frac{\Delta}{\alpha_2\omega_2 - \alpha_1\omega_1}\right|. \tag{10}$$

Synchronization is achieved when the effective coupling strength, here $\epsilon_{\text{eff}} = \beta p^2/2\gamma$, is larger than a function of the frequencies, i.e. $\epsilon_{\text{eff}} > |\Delta/(\alpha_2\omega_2 - \alpha_1\omega_1)|$. Further, the condition (10) depends on the amplitude of oscillation, p. Larger values of p lead to an onset of phase synchronization at smaller values of the coupling strength β. This is in contrast to the usual case of linear diffusive coupling, i.e. instead of using our control scheme (5) the two oscillators (x_1, y_1), (x_2, y_2) are coupled via introduction of the term $\beta(x_{2,1} - x_{1,2})$ into the equation for $\dot{x}_{1,2}$. With such diffusive coupling the synchronization threshold does not depend on the value of the amplitude p.

In Fig. 2 the locking (or synchronization) regions of system (7), as described by condition (10), are plotted in the parameter plane of effective coupling and natural frequency difference. By variations of different coupling schemes, i.e. uni- and bi-directional coupling, basically four different scenarios for the form of the locking regions can be found.

Obviously in the feedback coupling scheme, depending on the values of α_i, the locking regions are not defined by straight lines. Furthermore there are specific values of natural frequencies ($\alpha_2\omega_2 = \alpha_1\omega_1$), which arise from the singularities of (10) and for which synchronization can never be achieved. These special frequency values divide the parameter plane into different locking regimes. In some regions of Δ, synchronization is inhibited. In compensation, in other regimes of parameter space the synchronization is strongly promoted and the border of synchronization is moved towards smaller values of effective coupling strength.

Further indicated in Fig. 2 is also the phase difference of the two oscillators at the onset of synchronization. As a consequence of the cosine term in Eq. (8), the phase difference may be either 0° or 180°. Therefore, for the minimal coupling strength when synchronization sets in, the time lag between two nearby maxima of $x_i(t)$ is either 0 or $\pi/\bar{\Omega}$, where we have used the mean observed frequency

$$\bar{\Omega} = \langle\tfrac{1}{2}(\dot{\phi}_1 + \dot{\phi}_2)\rangle. \tag{11}$$

Consequently, at the onset of synchronization the two limit cycle oscillators are either fully synchronized or fully anti-synchronized.

Before the synchronization sets in, the observed frequency difference in the small coupling regime can be calculated in the case $\tau \ll 1$ as

$$\Delta\Omega = \frac{2\pi}{\int_0^{2\pi} \mathrm{d}\theta/\dot{\theta}} = \sqrt{\Delta^2 - \frac{\beta^2 p^4}{4\gamma^2}(\alpha_2\omega_2 - \alpha_1\omega_1)^2}. \tag{12}$$

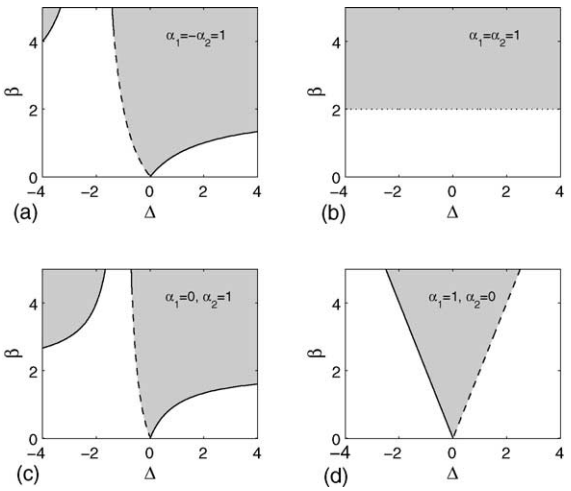

Fig. 2. Synchronization regions (gray) of the system (8) as described by (10) for different coupling scenarios and fixed $\omega_1 = 1$, $\gamma = 1$, $p = 1$. (a) $\alpha_1 = -\alpha_2 = 1$, (b) $\alpha_1 = \alpha_2 = 1$, (c) $\alpha_1 = 0$, $\alpha_2 = 1$, (d) $\alpha_1 = 1$, $\alpha_2 = 0$. Further indicated is the phase difference of both oscillators at the synchronization threshold, which is either $\theta^* = 0^\circ$ (solid line), $\theta^* = 180^\circ$ (dashed line), or undetermined, if the transition leads to oscillation death (dotted line).

We want to compare this analytical approximation with numerical simulations of Eq. (5). The phase of a limit cycle can be computed in the form

$$\phi_{1,2} = \arctan\left(\frac{y_{1,2}}{x_{1,2}}\right), \tag{13}$$

and the respective mean frequency as

$$\Omega_{1,2} = \lim_{T\to\infty} \frac{\phi_{1,2}(T) - \phi_{1,2}(0)}{T}. \tag{14}$$

The numerically calculated values of $\Delta\Omega$ can also be used to visualize the locking regions. A numerically computed synchronization surface is shown in Fig. 3. Compare this to the analytically derived Fig. 2c. In order to ensure synchronization, i.e. to avoid the multistability regime, we use the initial state in the middle of the two fixed points $\theta = \pi$ on the $\dot{\theta} = 0$ nullcline.

For parameter values of β in the transition regime near the bifurcation point, we find multistability. Depending on the initial states of the two Poincaré systems, they may synchronize or not. For example, starting above the nullclines in the phase space, the system is only able to reach a periodic, nonsynchronized state. Recall that such bistable behaviour is absent in the Kuramoto model. However, similar bistability is known to arise in two coupled oscillators with varying nonisochronicities [25].

3.1. Impossibility of synchronization with symmetrical coupling $\alpha_1 = \alpha_2$

We now study the special case of symmetrical coupling where $\alpha_1 = \alpha_2$. Inspection of Fig. 2 reveals the special role which is played by this coupling scheme because seemingly the synchronization threshold in this case is independent of the natural frequency difference between the oscillators. This result can also be found from Eq. (10). However, the picture is somewhat misleading because as we now show in this case it is impossible to synchronize the two oscillators at all. In order to calculate the mean observed frequency, defined in (11), of two Poincaré systems

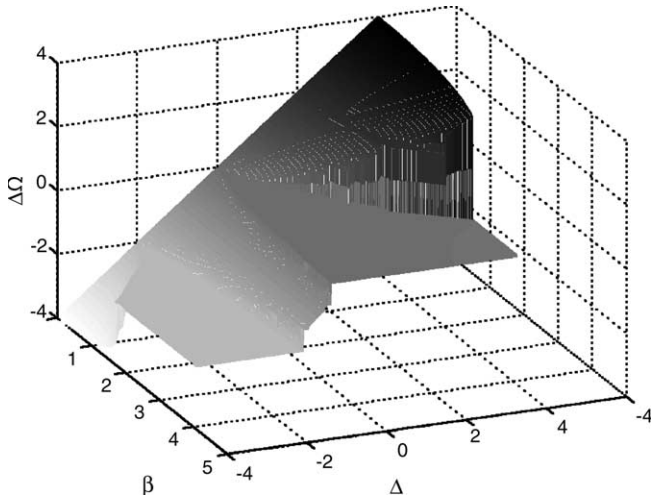

Fig. 3. Locking regions of (5) for uni-directional coupling $\alpha_1 = 0$, $\alpha_2 = 1$ in dependence on the coupling parameter β and the natural frequency difference Δ. $\gamma = 1$, $p = 1$, $\omega_1 = 1$.

(6) in the locked state, we require

$$\dot{\phi}_1 + \dot{\phi}_2 = \omega_1 + \omega_2 + u^*(\alpha_1\omega_1 + \alpha_2\omega_2). \tag{15}$$

After inserting the steady state value of the control variable u^*, Eq. (9), this results in

$$\bar{\Omega} = \frac{\omega_1 + \omega_2}{2} + \frac{\alpha_1\omega_1 + \alpha_2\omega_2}{\alpha_1\omega_1 - \alpha_2\omega_2}\frac{\Delta}{2}, \tag{16}$$

and replaces the usual formula $\bar{\Omega} = \bar{\omega}$ for two simply symmetrically coupled phase oscillators.

In the case of symmetrical coupling this has the implication that the mean observed frequency disappears

$$\alpha_1 = \alpha_2 \to \bar{\Omega} = \tfrac{1}{2}(\dot{\phi}_1 + \dot{\phi}_2) = 0. \tag{17}$$

Since in the synchronized state further $\Delta\Omega = 0$, we follow that $\Omega_1 = \Omega_2 = 0$ and the oscillators effectively stop to rotate. This result is also evident by going back to the feedback coupling scheme (Fig. 1). When $\alpha_1 = \alpha_2$, then both oscillators always obtain identical feedback. The only way in which then the observed frequencies can become identical is when they are controlled to zero, i.e. to oscillation death. This is also valid if u is introduced only in the second equation of (5), whereas for other oscillators in this case this does not hold, see Section 6.

3.2. Anti-symmetrical coupling, $\alpha_1 = -\alpha_2$

A special interest attains the scheme of anti-symmetrical coupling, where the feedback to the two oscillators has the same strength but opposite sign, $\alpha_1 = -\alpha_2$. Then, obviously the mean coupling strength disappears, $\bar{\alpha} = (\alpha_1 + \alpha_2)/2 = 0$, which leads with $\dot{u} = 0$ to the simplified phase Eq. (7)

$$\dot{\theta} = \Delta + \alpha\frac{\beta\bar{\omega}p^2}{\gamma}\cos(\theta). \tag{18}$$

Similar, the synchronization regime in the parameter space simplifies to

$$\alpha \frac{\beta \bar{\omega} p^2}{\gamma} > |\Delta|. \tag{19}$$

This expression for synchronization threshold resembles very much the usual synchronization of two coupled oscillators (see also Fig. 2a). However, note that even in this case there remain important differences. For example, synchronization sets in with a phase difference of either 0° or 180°.

We again calculate the mean frequency difference in the synchronized state

$$\dot{\phi}_1 + \dot{\phi}_2 = \omega_1 + \omega_2 + \frac{(\omega_1 - \omega_2)^2}{\omega_1 + \omega_2}, \tag{20}$$

which leads to

$$\bar{\Omega} = \frac{\omega_1^2 + \omega_2^2}{\omega_1 + \omega_2}. \tag{21}$$

Therefore, in the case of anti-symmetrical coupling the observed mean frequency in general is not the arithmetic mean of the natural frequencies.

It is also straightforward to calculate the forbidden frequency ratio, i.e. the ratio for which synchronization cannot be achieved in the scheme with antisymmetrical coupling. We are led to the condition $\bar{\omega} = 0$ or $\omega_2 = -\omega_1$. Therefore, synchronization cannot be achieved when both oscillators rotate in opposite direction with exactly the same frequency. This is similar to the Kuramoto phase model [1,23], however, here in the limit $\bar{\omega} \to 0$ the mean observed frequency goes to infinity $\bar{\Omega} \to \infty$ and not $\bar{\Omega} \to 0$.

4. Coupled van der Pol and Rössler oscillators

In the following we explore the feedback scheme for more complicated oscillator types. First, two structurally different oscillators are coupled: a regular – van der Pol – oscillator and a chaotic – Rössler – oscillator [28]. The equations describing the control scheme (same L and Q as in previous section) for PS of such oscillators are:

$$\begin{aligned}
\dot{x}_1 &= -\omega_1(1 + \alpha_1 u) y_1 - z_1, \\
\dot{y}_1 &= \omega_1(1 + \alpha_1 u) x_1 + a y_1, \\
\dot{z}_1 &= b - c z_1 + x_1 z_1, \\
\dot{x}_2 &= y_2, \\
\dot{y}_2 &= -(\omega_2(1 + \alpha_2 u))^2 x_2 + \varepsilon(p^2 - x_2^2) y_2, \\
\dot{u} &= -\gamma u + \beta x_1 x_2,
\end{aligned} \tag{22}$$

where x_1, y_1, z_1 are the variables of the Rössler oscillator, x_2, y_2 are the variables of the van der Pol oscillator. u is again the control variable added in both subsystems, $\alpha_{1,2}$, β and γ are control parameters. We set $\beta = \gamma = 1$. For the van der Pol oscillator we choose the following set of parameters: $\omega_2 = 1$, $\varepsilon = 0.01$, and $p = 4$. The parameters of the Rössler oscillator will be chosen as: $a \in [0.15 : 0.2]$, $b = 0.1$, $c = 8.5$, and $\omega_1 = 1$ [29]. For these values the topology of the chaotic Rössler attractor is rather simple, i.e. phase-coherent, and one can introduce the phase in the form:

$$\phi_1 = \arctan\left(\frac{y_1}{x_1}\right). \tag{23}$$

For chosen ε the phase trajectory of the van der Pol oscillator regularly monotonously oscillates around the origin, so we can use a similar definition of the phase

$$\phi_2 = -\arctan\left(\frac{y_2}{x_2}\right). \tag{24}$$

In order to test for the existence of phase synchronization between Rössler and van der Pol oscillators, we use as in the previous chapters two criteria: PS sets in

(i) if the mean frequencies of both coupled subsystems become equal (frequency locking):

$$\Omega_2 = \Omega_1, \tag{25}$$

where the frequencies are defined as:

$$\Omega_{1,2} = \lim_{T\to\infty} \frac{\phi_{1,2}(T) - \phi_{1,2}(0)}{T}, \tag{26}$$

(ii) and if the phase difference is bounded:

$$|\phi_2 - \phi_1| \leq \text{const}. \tag{27}$$

We consider two types of unidirectional (drive-response) feedback coupling:

(a) we control the characteristic time of the Rössler oscillator ($\alpha_2 = 0$ in (22)) (Fig. 4),
(b) or we control the characteristic time of the van der Pol oscillator ($\alpha_1 = 0$ in (22)) (Fig. 5). In both cases there are critical values of the feedback control parameters $\alpha^*_{1,2}$ corresponding to the onset of synchronization.

First, we study the case where the van der Pol oscillator is the drive system and the Rössler oscillator is the controlled response system. We set $a = 0.15$, so that the chaotic attractor of the Rössler oscillator is phase-coherent. To illustrate the transition to PS, we plot the mean frequency difference and the three largest Lyapunov exponents versus the control parameter α_1 (Fig. 4a), as well as a bifurcation diagram (Fig. 4b). We find that PS occurs at $\alpha^*_1 = 0.00123$. There the behavior of the Rössler oscillator remains chaotic but with the mean observed frequency Ω_1 equal to the frequency ω_2 of the van der Pol oscillator. A similar situation of chaotic frequency locking was observed in [30,31], where effects of PS were observed in a chaotic system forced by an external periodic signal. In contrast to this, our interacting subsystems are autonomous and therefore without coupling two zero Lyapunov exponents exist. In this case the transition to phase synchronization can be analyzed by means of the Lyapunov exponents. As it can be seen from Fig. 4a the frequency locking occurs approximately (shortly after) at that value of α_1 for which one of the zero Lyapunov exponents becomes negative. Our numerical experiments (for other values of a) show that usually the behavior of the controlled Rössler oscillator remains chaotic. But there are also intervals of α_1 where the behavior of the Rössler oscillator becomes periodic (Fig. 4). Thus, very small coupling allows to control chaotic systems in such a way that (i) we can govern the mean frequency of chaotic oscillations and (ii) we can get periodic oscillations too.

In the second case of unidirectional feedback coupling, the Rössler oscillator is the drive system and the van der Pol oscillator is the controlled response system. Here we analyze not only the phase-coherent chaotic attractor ($a = 0.16$) but also the funnel attractor ($a = 0.24$). In the latter case the topology of the attractor is much more complex and the phase cannot be defined as in (23). Thus we introduce another phase definition [32]

$$\phi_1 = \arctan\left(\frac{\dot{y}_1}{\dot{x}_1}\right), \tag{28}$$

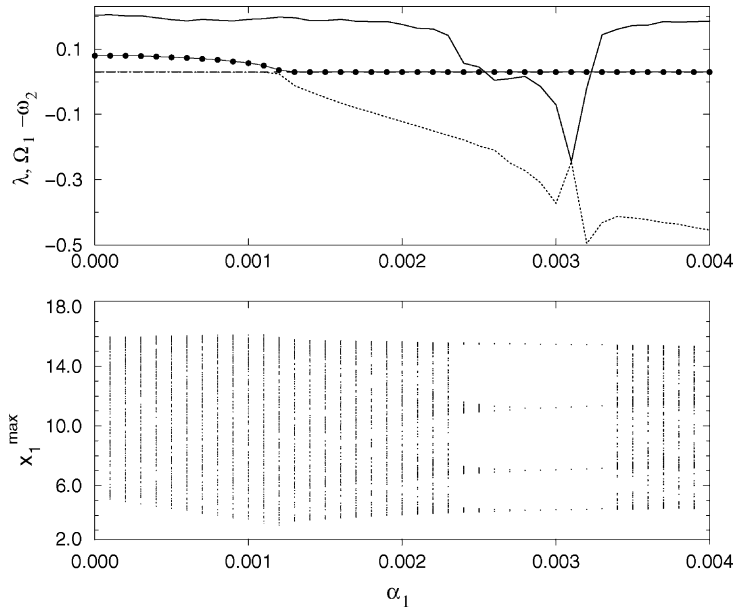

Fig. 4. Transition to phase synchronization for unidirectionally ($\alpha_1 = 0$ in (22)) feedback coupled Rössler and van der Pol oscillators. The van der Pol oscillator is the drive system and the Rössler oscillator is the controlled response system. The mean observed frequency of the Rössler oscillator Ω_1 at $\alpha_1^* = 0.00123$ becomes equal to the frequency of the van der Pol oscillator ω_2. (a) The three largest Lyapunov exponents, one of which is always zero, and the difference of the mean observed frequencies $\Omega_1 - \omega_2$ (circles) vs. the control parameter α_1. (b) Maxima of x_1 vs. α_1.

and use the same two criteria (25) and (27) as in the previous case. We plot in Fig. 5a the difference of the mean observed frequencies $\Omega_1 - \Omega_2$ vs. the feedback control parameter α_1 for different values of a. In all cases PS occurs at some critical values α_2^*, but with increasing of a a larger value α_2^* is needed to achieve the locking. The onset of PS is well manifested in the bifurcation diagrams (Fig. 5b–d). One can see that with increasing of α_2 the interval l of possible maximum values of x_2 becomes larger at first. But at the transition point to synchronization a strong shrinking of the interval l is observed. That means that the variables x_2 and y_2 become localized in a relatively small area.

We have also performed numerical simulations where the van der Pol and the Rössler oscillator are mutually coupled by feedback ($\alpha_{1,2} \neq 0$). The effect of both regular and chaotic PS has been observed there as well.

5. Two coupled Rössler oscillators

In this section we will demonstrate feedback control of chaotic phase synchronization for two coupled Rössler oscillators:

$$\begin{aligned}
\dot{x}_{1,2} &= -\omega_{1,2}(1 + \alpha_{1,2}u)y_{1,2} - z_{1,2},\\
\dot{y}_{1,2} &= \omega_{1,2}(1 + \alpha_{1,2}u)x_{1,2} + ay_{1,2},\\
\dot{z}_{1,2} &= b - cz_{1,2} + x_{1,2}z_{1,2},\\
\dot{u} &= -\gamma u + \beta x_1 x_2,
\end{aligned} \tag{29}$$

where $x_{1,2}$, $y_{1,2}$, $z_{1,2}$ are the variables of the first and second Rössler oscillator, respectively. We set: $\beta = \gamma = 1$, $a = 0.15$, $b = 0.1$, $c = 8.5$, $\omega_1 = 0.98$, and $\omega_2 = 1.02$. Hence, for both oscillators the phase definitions (23) can be used. The existence of PS between Rössler oscillators is tested again by the criteria (25) and (27).

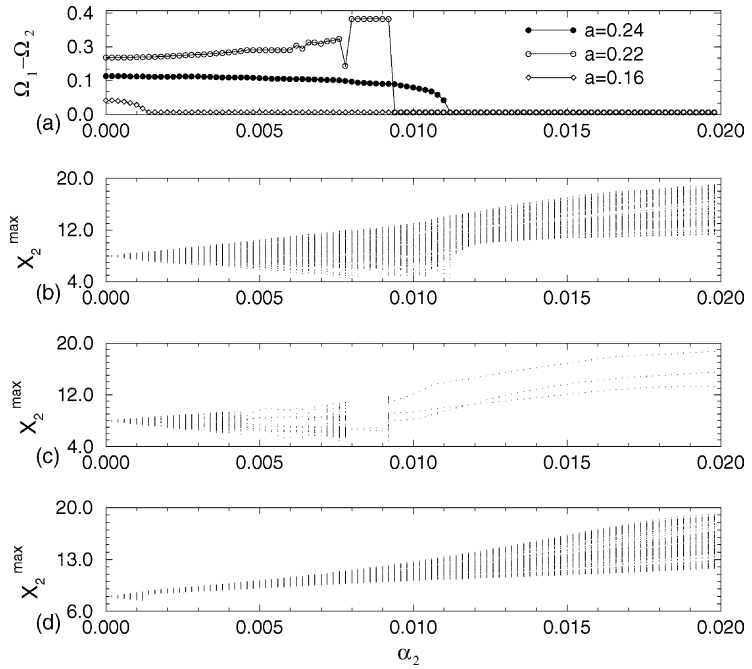

Fig. 5. Transition to phase synchronization for unidirectionally ($\alpha_2 = 0$ in (22)) feedback coupled Rössler and van der Pol oscillators. The Rössler oscillator is the drive system and the van der Pol oscillator is the controlled response system. The observed frequency of the van der Pol oscillator Ω_2 after some α_2^* becomes equal to the mean frequency of the Rössler oscillator Ω_1. (a) The difference of the mean observed frequencies $\Omega_1 - \Omega_2$ (circles) vs. control parameter α_2. (b–d) Maximal values of x_2 vs. α_2. The parameters are: (b) $a = 0.24$, (c) $a = 0.22$ (for $a = 0.22$ attractor in Rössler oscillator is periodic), and (d) $a = 0.16$.

We compute the spectrum of the Lyapunov exponents (Fig. 6a), the mean frequency difference (Fig. 6a), and the evolution of the phase difference (Fig. 6b). PS sets in at the essentially small coupling $\alpha_1^* = -\alpha_2^* \approx 0.000415$. Note that shortly before PS one of the zero Lyapunov exponents becomes negative. With increasing of α_1, the frequency difference decreases smoothly (without jump), i.e. a soft transition to PS takes place. This is manifested in the evolution of the phase difference, namely for the control parameters close to the critical value α_1^* phase locking at large time intervals is observed (Fig. 6b). In order to estimate the critical coupling strength corresponding to the appearance of synchronization, we make a transformation to cylindrical coordinates: $x_{1,2} = \rho_{1,2}\cos\phi_{1,2}$ and $y_{1,2} = \rho_{1,2}\sin\phi_{1,2}$. Then for the feedback coupled oscillators (29), the averaged equation for the difference $\theta = \psi_2 - \psi_1$ of slow phases $\psi_{1,2} = \phi_{1,2} - \omega_0 t$ reads as:

$$\ddot{\theta} + \gamma\dot{\theta} + \alpha\beta\rho_1\rho_2 \sin\theta = \gamma\Delta, \tag{30}$$

where we have set $\alpha = \alpha_1\omega_1 = -\alpha_2\omega_2$. If we neglect the fluctuations of the amplitude, Eq. (30) has the stationary solution:

$$\bar{\theta} = \arcsin\left(\frac{\gamma\Delta}{\alpha\beta\rho_1\rho_2}\right). \tag{31}$$

This state exists and is stable if:

$$\left|\frac{\Delta}{\rho_1\rho_2}\right| < \alpha, \tag{32}$$

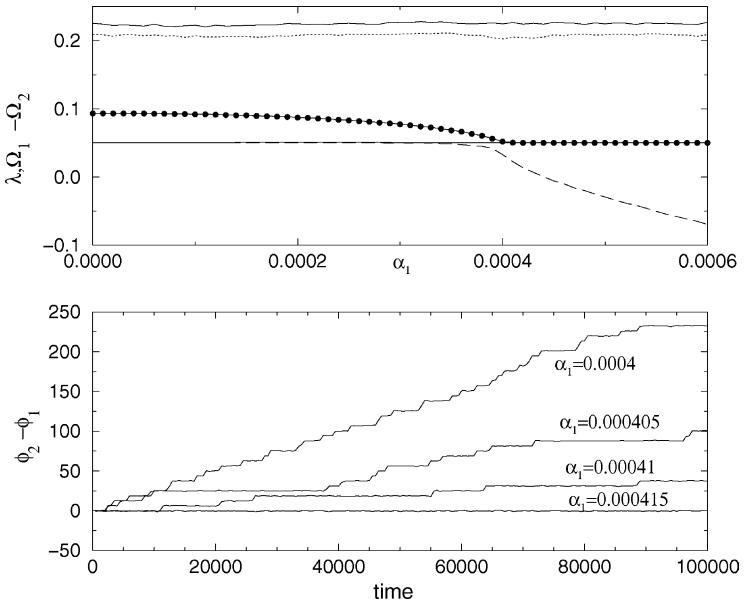

Fig. 6. Synchronization of two coupled Rössler oscillators (29). The parameters are: $a = 0.15$, $b = 0.1$, $c = 8.5$, $\omega_1 = 0.98$, $\omega_2 = 1.02$, $\alpha_1 = -\alpha_2$, and $\beta = \gamma = 1$. (a) The four largest Lyapunov exponents and the difference of the mean observed frequencies $\Omega_1 - \Omega_2$ (circles) vs. the control parameter α_1. (b) Difference of the phases $\phi_2 - \phi_1$ for nonsynchronous ($\alpha_1 = 0.0004; 0.000405; 0.00041$) and synchronous ($\alpha = 0.000415$) regimes.

with $\beta = \gamma = 1$. Let us compare the effectiveness of the proposed coupling scheme with respect to the diffusive coupling usually considered. In the latter case the equations of motions for two diffusively coupled Rössler oscillators are (see [33]):

$$\begin{aligned} \dot{x}_{1,2} &= -\omega_{1,2} y_{1,2} - z_{1,2} + \alpha(x_{2,1} - x_{1,2}), \\ \dot{y}_{1,2} &= \omega_{1,2} x_{1,2} + a y_{1,2}, \\ \dot{z}_{1,2} &= b - c z_{1,2} + x_{1,2} z_{1,2}. \end{aligned} \tag{33}$$

The equation for the phase difference can be recast in the form:

$$\dot{\theta} - \frac{\alpha}{2} \frac{\rho_1^2 + \rho_2^2}{\rho_1 \rho_2} \sin\theta = \Delta. \tag{34}$$

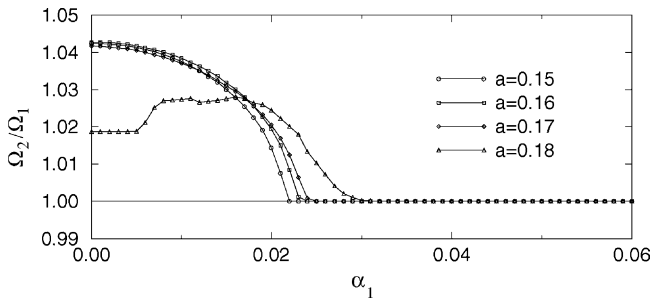

Fig. 7. Synchronization of two coupled Rössler oscillators (38). The ratio of the mean observed frequencies Ω_2/Ω_1 vs. the control parameter α_1. The parameters of the individual oscillators are the same as in Fig. 6.

The stable stationary state

$$\bar{\theta} = -\arcsin \frac{2\Delta\rho_1\rho_2}{\alpha(\rho_1^2+\rho_2^2)} \tag{35}$$

exists in the range

$$\alpha > \frac{|2\Delta\rho_1\rho_2|}{\rho_1^2+\rho_2^2}. \tag{36}$$

If we take not strongly different oscillators (i.e., $\rho_1 \approx \rho_2$) this range is reduced to:

$$\alpha > |\Delta|. \tag{37}$$

Therefore, by equivalent parameters of the interacting oscillators, the synchronization range for the feedback coupling (Eq. (29)) is $p^2\alpha/\gamma = \rho_1\rho_2\alpha/\gamma$ times larger than for the diffusive coupling (Eq. (33)). This estimation is in very good agreement with our numerical results.

We have also analyzed the synchronization transitions for the simplest case of a linear operator L. For $\alpha \gg 1$ the filtered control variable u can be expressed by $\sin(\phi_2 - \phi_1)$, where the phases $\phi_{1,2}$ are introduced by (23). Then Eq. (29) can be rewritten as:

$$\begin{aligned}
\dot{x}_{1,2} &= -\omega_{1,2}[1+\alpha_{1,2}\sin(\phi_{2,1}-\phi_{1,2})]y_{1,2} - z_{1,2},\\
\dot{y}_{1,2} &= \omega_{1,2}[1+\alpha_{1,2}\sin(\phi_{2,1}-\phi_{1,2})]x_{1,2} + ay_{1,2},\\
\dot{z}_{1,2} &= b - cz_{1,2} + x_{1,2}z_{1,2}.
\end{aligned} \tag{38}$$

The dependency of the mean frequency ratio Ω_2/Ω_1 on the parameter $\alpha_1 = -\alpha_2$ for different a shows the onset of PS again for a very small coupling strength (Fig. 7).

In Fig. 8 we have analyzed the transition to synchronization in the two coupled Rössler systems for different coupling schemes. Fastest synchronization is achieved for antisymmetrical ($\alpha_1 = -\alpha_2$) coupling. For unidirectional coupling locking can also be obtained, but not for symmetrical coupling ($\alpha_1 = \alpha_2$).

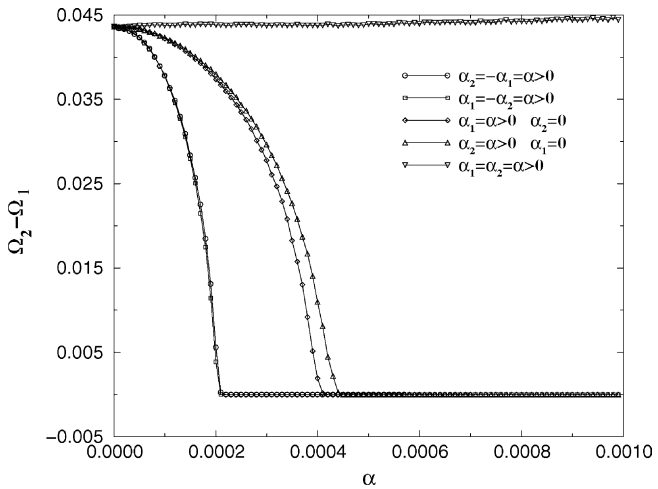

Fig. 8. Synchronization of two coupled Rössler oscillators (38) for different coupling schemes. Plotted is the frequency of the mean observed frequencies $\Omega_2 - \Omega_1$ vs. the control parameter α. The coupling parameters α_1 and α_2 are taken as explained in the figure. The parameters of the individual oscillators are the same as in Fig. 6.

6. Coupled foodweb models

In this section we apply the automatic phase synchronization to foodweb models from ecology. First, we study the synchronization of two coupled limit-cycle Lotka–Volterra [34] systems

$$\begin{aligned}
\dot{x}_{1,2} &= a x_{1,2}\left(\tfrac{1-x_{1,2}}{K}\right) - k f_H(x_{1,2}, y_{1,2}),\\
\dot{y}_{1,2} &= -b_{1,2}(1+\alpha_{1,2}u)\, y_{1,2} + k f_H(x_{1,2}, y_{1,2}),\\
\dot{u} &= -\gamma u + \beta y_1 y_2.
\end{aligned} \tag{39}$$

Here, $x_{1,2}$ denotes the prey and $y_{1,2}$ the predator species, a and $b_{1,2}$ are the birth and death rates, K is the prey carrying capacity, k the predation rate and κ the half saturation constant of the Holling type II functional response $f_H(x, y) = xy/(1+\kappa x)$. Throughout this section we use the parameter values $a = 1, k = 3, K = 3, \kappa = 1$. The two oscillators are nonidentical and vary in the value of predator death rates $b_1 = 1.0$ and $b_2 = 0.95$.

The control variable u is introduced into the model as in the previous models. Ecologically, quadratic forms Q of Eq. (4) can arise very naturally as Lotka–Volterra interactions. Here, u represents a species that is affected and grows only in the presence of the predator y_i of both sites, 1 and 2, and has a mortality γ which represents the filter L. However, the predators are not directly influenced by u, i.e. both species are in commensalism. Instead, the death rates $b_{1,2}$ are modified by the abundance of the species u.

Without coupling, system (39) is well known to exhibit limit cycle oscillations with a frequency roughly determined by $\omega_i = \sqrt{ab_i}$. Nevertheless, feedback control is able to achieve synchronization (see Fig. 9). Depending on the coupling scheme synchronization may or may not be achieved. Note that in Fig. 9 the control parameter α is varied in the whole range from negative to positive values.

Further, we want to stress that in system (39) synchronization can be achieved even in the symmetrical scheme where the values of α are identical, i.e. $\alpha_1 = \alpha_2 = \alpha$. This is astonishing because then the parameters in the model (and consequently also the natural frequencies) are modified by exactly the same amount $b_i(1+\alpha u)$. This is in contrast to the simple theory with two Poincaré oscillators Eq. (5) where identical α_i only lead to oscillation death (see Section 3.1). Of course, in the foodweb case u is only introduced into the second equation of (39) and not also to $\dot{x}$ as in (5). However, the principal behaviour of the Poincaré system remains unchanged even if u is only introduced into the second equation, i.e. symmetrical coupling only results in oscillation death. Similar behaviour, i.e. synchronization in symmetrical coupling, was also observed in the Rössler system, if u is affecting only the second equation of (29).

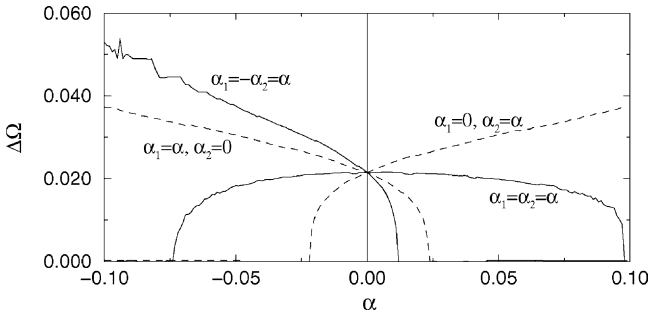

Fig. 9. Transition to synchronization for two limit cycle Lotka–Volterra models coupled via feedback loop. (Solid lines) Bidirectional coupling with either symmetric ($\alpha_1 = \alpha_2 = \alpha$) or antisymmetric ($\alpha_1 = -\alpha_2 = \alpha$) coupling scheme; (dashed lines) unidirectional coupling ($\alpha_1 = 0$ or $\alpha_2 = 0$).

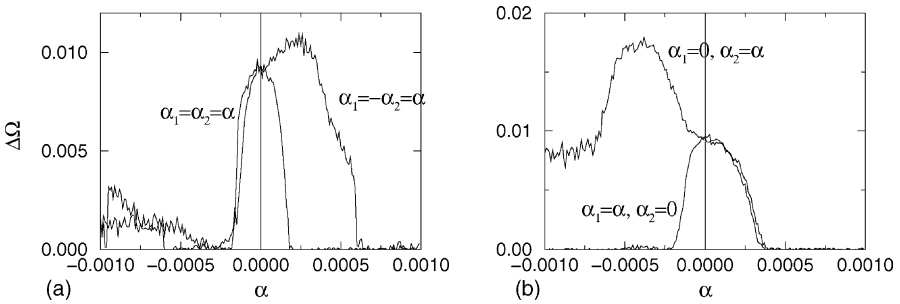

Fig. 10. Transition to synchronization for two chaotic foodweb models coupled via feedback loop. (a) Bidirectional coupling with either symmetric ($\alpha_1 = \alpha_2 = \alpha$) or antisymmetric ($\alpha_1 = -\alpha_2 = \alpha$) coupling scheme; (b) unidirectional coupling ($\alpha_1 = 0$ or $\alpha_2 = 0$).

Next, we study feedback control in a model for chaotic predator–prey cycles, which has been proposed in [3,35]

$$\begin{aligned}
\dot{x}_{1,2} &= a x_{1,2} - e f_H(x_{1,2}, y_{1,2}),\\
\dot{y}_{1,2} &= -b_{1,2}(1 + \alpha_{1,2} u) y_{1,2} + e f_H(x_{1,2}, y_{1,2}) - g\, y_{1,2}\, z_{1,2},\\
\dot{z}_{1,2} &= -c(z_{1,2} - z_0) + g\, y_{1,2}\, z_{1,2},\\
\dot{u} &= -\gamma u + \beta y_1 y_2.
\end{aligned} \tag{40}$$

This model describes a three trophic "vertical" food chain where the vegetation x is consumed by herbivores y which themselves are preyed upon by the top predator z. In the absence of interspecific interactions the dynamics is linearly expanded around the steady state $(0, 0, z_0)$ with coefficients a, $b_{1,2}$ and c that represent the respective nett growth and death rates of each species. Predator–prey and consumer–resource interactions are incorporated into the equations via either the Lotka–Volterra term xy, or the Holling type II term $f_h(x, y) = xy/(1 + \kappa x)$ with strengths set by the coefficients e and g. Despite their minimal structure, the above equations might sketch the major ecological transfers involved in the Canadian lynx-hare-vegetation foodweb [3,35].

For simulation runs reported here, parameter values are taken as in [3,35] ($a = 1, c = 10, e = 0.2, g = 1, \kappa = 0.05, z_0 = 0.006$). The parameter mismatch between the two oscillators is given by $b_1 = 0.96$; $b_2 = 0.98$. In this parameter range the model shows phase coherent chaotic dynamics, where the trajectory rotates with nearly constant frequency in the (x, y)-plane but with chaotic dynamics that appear as irregular spikes in the top predator z. This behaviour of the foodweb model is reminiscent to the Rössler system (29) and therefore one might expect similar synchronization properties in both systems.

Simulation results are shown in Fig. 10. Also in the chaotic ecological model synchronization in phase can be obtained. However, we find a rich behaviour. In the unidirectional coupling scheme for positive α, synchronization is achieved in both cases. For negative α synchronization is achieved only in the case $\alpha_2 = 0$ (see Fig. 10b).

In the bidirectional coupling schemes, depicted in Fig. 11a, synchronization is found in all cases if the absolute value of α is sufficiently large. In the antisymmetric coupling scheme, e.g. $\alpha_1 = -\alpha_2 = \alpha$, for positive values of α the transition to synchronization is characterized by the fact that with the onset of coupling the frequency difference is first increasing with a maximal difference for intermediate values (here $\alpha \approx 0.00025$). Whereas frequencies become attracted and locking arises only for larger values of the coupling strength. Similar behaviour is known to arise also in two diffusively coupled foodweb models and has been called anomalous phase synchronization [36].

7. Coupled Rössler and Lorenz oscillators

Now we will apply the automatic phase synchronization to the coupled Rössler and Lorenz [27] oscillators, i.e. chaotic oscillators with a well pronounced difference in topology (see Sections 4 and 5). The model is:

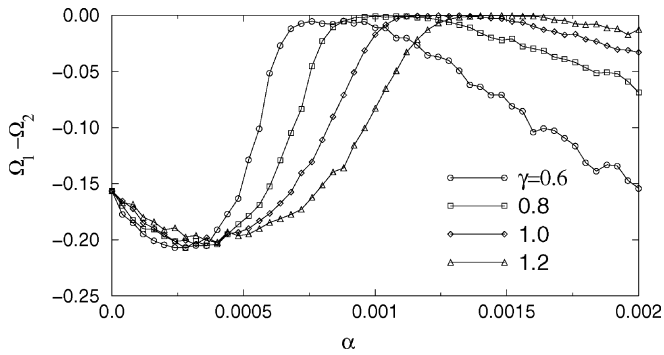

Fig. 11. Synchronization of coupled Rössler and Lorenz oscillators (41). The parameters are: $a = 0.15$, $b = 0.1$, $c = 8.5$, $\omega = 0.98$, $\sigma = 10$, $r = 28$, $b = 8/3$, $\alpha_1 = -\alpha_2 = \alpha$, and $\beta = \gamma = 1$. The difference of the mean observed frequencies $\Omega_1 - \Omega_2$ vs. the control parameter α.

$$\begin{aligned}
\dot{x}_1 &= \tau(-\omega(1+\alpha_1 u)y_1 - z_1),\\
\dot{y}_1 &= \tau(\omega(1+\alpha_1 u)x_1 + a y_1),\\
\dot{z}_1 &= b - c z_1 + x_1 z_1,\\
\dot{x}_2 &= \sigma(y_2 - x_2),\\
\dot{y}_2 &= r x_2 - y_2 - x_2 z_2,\\
\dot{z}_2 &= (1+\alpha_2 u)(-b z_2 + x_2 y_2),\\
\dot{u} &= -\gamma u + x_1 z_2,
\end{aligned} \tag{41}$$

where $x_{1,2}$, $y_{1,2}$, $z_{1,2}$ are the variables of the Rössler and Lorenz oscillators, respectively. The parameters a, b, c and the phase of the Rössler oscillator are the same as in the previous case; $\omega = 0.98$, $\tau = 8.3$, $\sigma = 10$, $r = 28$, and $b = 8/3$ and the phase of the Rössler oscillator is measured as before. The phase of the Lorenz oscillator is calculated as $\theta = \arctan((z_2 - 27)/(\sqrt{x_2^2 + y_2^2} - 12))$ [31]. In Fig. 11 we present results of the transition to chaotic PS between Rössler and Lorenz oscillators. One can see an interval of α where PS occurs.

In summary, using the proposed automatic scheme we are able to achieve chaotic PS between oscillators with a strong difference in their topology. Here, we mostly concentrated on the case of phase coherent oscillators, where a phase is easily defined. However at the end of Section 4, synchronization was established between a limit-cycle van der Pol oscillator and a funnel Rössler oscillator. Thus, we demonstrated that our method even works for phase noncoherent chaotic oscillators. Thus, we conclude that the automatic control of synchronization is a very robust method. Further investigation of our technique applied to noncoherent oscillators will be a interesting project for future research.

8. Principles of automatic synchronization in networks of coupled oscillators

It is easy to extent the control scheme proposed for two coupled oscillators to a network of oscillators. Let us consider an ensemble of arbitrary regular or chaotic oscillators given by the system:

$$\dot{x}_j = F_j(x_j, \omega_j), \qquad j = 1, \ldots, N, \tag{42}$$

where x_j and F_j are n-vectors, ω_j are parameters defining the time dependence rate of oscillations $x_j(t)$ and N is the number of oscillators.

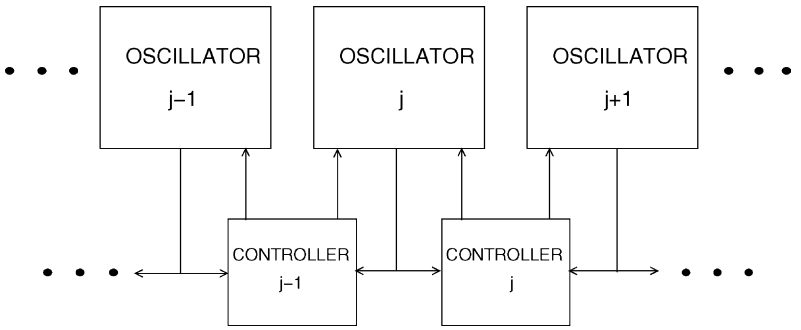

Fig. 12. Local feedback coupling in a chain of oscillators.

In order to synchronize these systems, we apply a feedback control between all of them in the following form:

$$\begin{aligned} &\dot{x}_j = F_j(x_j, \omega_j + \alpha_j u_j), \\ &L u_j = Q_j(x_1, \ldots, x_N), \qquad j = 1, \ldots, N, \end{aligned} \tag{43}$$

where L is again a linear operator acting as a low-pass filter; the function $Q_j(x_1, \ldots, x_N)$ is:

$$Q_j(x_1, \ldots, x_N) = \sum_{k=1, k\neq j}^{N} Q_k(x_j, x_k), \tag{44}$$

where Q_k is a quadratic form $Q_k = x_j^T H x_k$ which characterizes the coupling between the jth and the kth oscillators.

Now we study whether the control variable $u_j(t)$ added to each oscillator can provide a synchronous behavior between the interacting elements. Fig. 12 presents a simple scheme which roughly describes the proposed coupling technique.

We demonstrate the method of feedback control for PS for ensembles of (i) locally coupled regular oscillators (Section 9), (ii) locally coupled chaotic oscillators (Section 10), and (iii) globally coupled chaotic oscillators (Section 11).

9. Synchronization of locally coupled regular oscillators

As the simplest case, we consider feedback control of PS in an ensemble of *locally* mutually coupled Poincaré systems:

$$\begin{aligned} &\dot{x}_j = -(\alpha_j u_j + \omega_j) y_j - \lambda(x_j^2 + y_j^2 - p^2) x_j, \\ &\dot{y}_j = (\alpha_j u_j + \omega_j) x_j - \lambda(x_j^2 + y_j^2 - p^2) y_j, \\ &\dot{u}_j = -u_j + \beta_{j+1} x_j y_{j+1} + \beta_{j-1} x_j y_{j-1}, \end{aligned} \tag{45}$$

where $j = 1, \ldots, N$, ω_j are the frequencies, p is the amplitude of oscillations and $\lambda > 0$ is a damping parameter of the oscillators, u_j is the control variable, α_j and β_j are the parameters of the jth controller. We assume free-end boundary conditions: $\beta_0 = \beta_{N+1} = 0$. For the quadratic form Q_j we take the simplest form of coupling with nearest neighbors

$$Q_j = \beta_{j+1} x_j y_{j+1} + \beta_{j-1} x_j y_{j-1}. \tag{46}$$

In this example we take the linear operator L in the form $L = \mathrm{d}/\mathrm{d}t + 1$. Using polar coordinates $x_j = \rho_j \cos\phi_j$, $y_j = \rho_j \sin\phi_j$, we rewrite (45) in the form:

$$\begin{aligned} &\dot\rho_j = \lambda\rho_j(p^2 - \rho_j^2),\\ &\dot\phi_j = \alpha_j u_j + \omega_j,\\ &\dot u_j = -u_j + \beta_{j+1}\rho_j\rho_{j+1}\cos\phi_j \sin\phi_{j+1} + \beta_{j-1}\rho_j\rho_{j-1}\cos\phi_j\sin\phi_{j-1}, \qquad j = 1,\dots,N. \end{aligned} \tag{47}$$

We take a linear increasing distribution of individual frequencies $\omega_j = \omega_1 + \Delta(j-1)$, and $\alpha_j = \alpha$, $\beta_j = \beta$. Then by introducing the phase difference variable $\theta_j = \phi_j - \phi_{j+1}$, $\hat\alpha = \alpha\beta/2$ and averaging the system (47), we obtain:

$$\ddot\phi_1 + \dot\phi_1 = \omega_1 + \hat\alpha p^2 \sin\theta_1, \tag{48}$$

$$\ddot\theta_j + \dot\theta_j = \Delta + \hat\alpha p^2(\sin\theta_{j+1} - 2\sin\theta_j + \sin\theta_{j-1}), \qquad j = 1,\dots,N-1 \tag{49}$$

with the boundary conditions: $\theta_0 = \theta_N = 0$. These equations describe the synchronization regime in an ensemble of coupled Poincaré systems. The existence of a PS regime is defined by a stable steady state in (49). This state $(\bar\theta_1,\dots,\bar\theta_j,\dots,\bar\theta_{N-1})$ in system (49) corresponds to a regime of global synchronization in the chain. Hence, the system of equations for the stationary phase differences $\bar\theta_n$ can be written as:

$$\begin{aligned} &\Delta + \hat\alpha p^2(\sin\bar\theta_2 - 2\sin\bar\theta_1) = 0,\\ &\Delta + \hat\alpha p^2(\sin\bar\theta_{j+1} - 2\sin\bar\theta_j + \sin\bar\theta_{j-1}) = 0, \qquad j = 2,\dots,N-2,\\ &\Delta + \hat\alpha p^2(\sin\bar\theta_N - 2\sin\bar\theta_{N-1}) = 0. \end{aligned} \tag{50}$$

The distribution of $\bar\theta_j$ is [37]:

$$\sin\bar\theta_j = \frac{\Delta}{2\hat\alpha p^2}(Nj - j^2). \tag{51}$$

It follows from (51) that the system (49) can have 2^{N-1} steady states. But only one of them ($\bar\theta_j \in [-\pi/2;\pi/2]$ for all $j = 1,\dots,N-1$) can be stable. As the frequency mismatch Δ is increased, the condition for the existence of steady states

$$\left|\frac{\Delta}{2\hat\alpha p^2}(Nj - j^2)\right| < 1 \tag{52}$$

is violated first for $j = N/2$ at even N, i.e. for the middle element in the chain. Thus, the condition for the existence of a stable steady state in the N-element chain is given by the inequality

$$\left|\frac{\Delta N^2}{8\hat\alpha p^2}\right| < 1. \tag{53}$$

The frequency of global synchronization Ω_s may be determined from Eq. (49), such that

$$\Omega_s = \omega_1 + \tfrac{1}{2}\Delta(N-1). \tag{54}$$

Then the frequencies for all elements are equal to the mean frequency of the elements in the ensemble. With an increase of the frequency mismatch Δ (or decrease of the coupling α), a loss of global synchronization takes place. For a long chain two synchronization clusters occur, i.e. the chain is divided into two clusters each of size $(N/2)$, both consisting of mutually synchronized oscillators. Further increase of Δ (decrease of α) leads to a sequence of destruction of the one cluster structure of the synchronized elements and to the appearance of another structure. This sequence obtained in numerical experiments is presented in Fig. 13. From this figure we recognize two types of transitions between cluster structures. In the first type a "hard" transition without intermediate structures occurs from the state with n $(n+1)$ clusters to the state with $n+1$ (n) clusters (see, for example, the interval $[0.019 : 0.023]$).

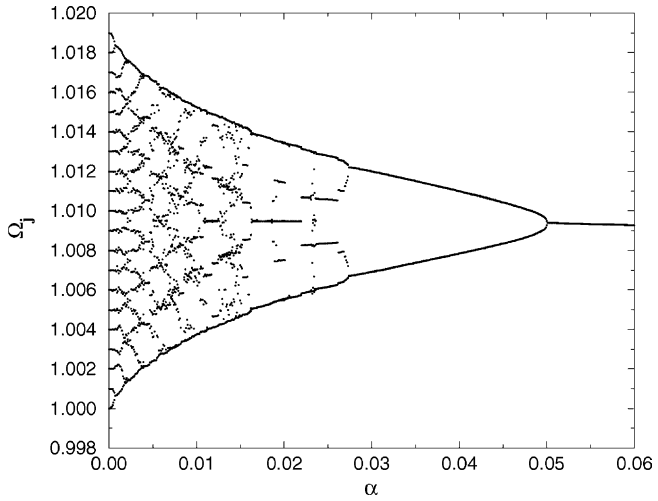

Fig. 13. Observed frequencies Ω_j in a chain of Poincaré systems (Eq. 45) with linear distribution of individual frequencies versus α. $N = 20$, $p = 1$, $\omega_1 = 0.98$, $\Delta = 0.001$.

In the second type, a "soft" transition happens with a smooth transition of intermediate structures one into the other. As follows from Fig. 13, the theoretically and numerically obtained condition of global synchronization and the global synchronization frequency are in very good agreement.

10. Synchronization of locally coupled chaotic oscillators

Now we will demonstrate feedback control of chaotic PS in ensembles of *locally* coupled Rössler oscillators:

$$\begin{aligned}
\dot{x}_j &= -(\omega_j + \alpha_j u_j) y_j - z_j, \\
\dot{y}_j &= (\omega_j + \alpha_j u_j) x_j + a y_j, \\
\dot{z}_j &= b - c z_j + x_j z_j, \\
\dot{u}_j &= -\gamma_j u_j + \beta_{j+1} x_j y_{j+1} + \beta_{j-1} x_j y_{j-1}, \qquad j = 1, \ldots, N.
\end{aligned} \tag{55}$$

We set: $a = 0.15$, $b = 0.1$, $c = 8.5$, $\alpha_j = \alpha$, $\gamma_j = \beta_j = 1$. Like in the Poincaré systems, we introduce a gradient distribution of natural frequencies $\omega_j = \omega_1 + \Delta(j-1)$ with $\omega_1 = 0.98$, and $\Delta = 0.0001$. Another variant considered below is a random distribution of natural frequencies in the range $[\omega_1, \omega_1 + \Delta(N-1)]$. We again assume free-end boundary conditions: $\beta_0 = \beta_{N+1} = 0$. The control scheme Q_j is the same as in the previous section and $L = \mathrm{d}/\mathrm{d}t + \gamma_j$. As a condition of synchronization, we again consider the coincidence of the observed partial frequencies defined according to (26).

We have performed numerical simulations with a chain of 100 elements with a linear and a random distribution of the individual frequencies. For each element for different α the frequency Ω_j has been calculated. We find that in both cases all frequencies Ω_j become equal with increasing coupling α, which means global chaotic PS sets in.

We have also analyzed synchronization transitions in the simplest case of a linear operator L. For $\gamma_j \gg 1$ the filtered control variable u_j can be expressed as

$$u_j = \sin(\phi_{j+1} - \phi_j) + \sin(\phi_{j-1} - \phi_j), \tag{56}$$

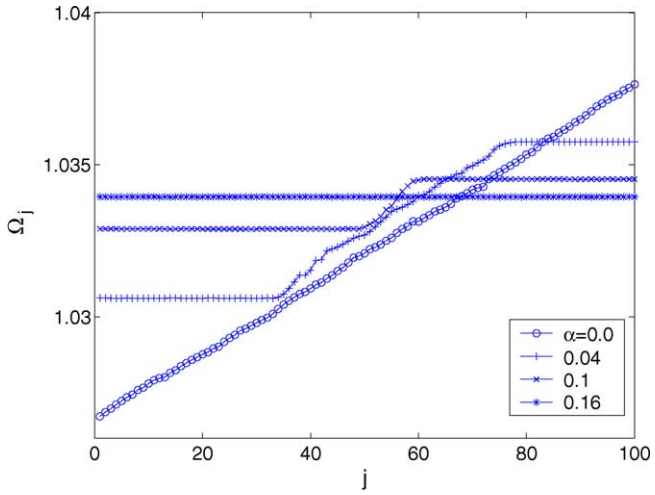

Fig. 14. Mean frequencies Ω_j in a chain of Rössler oscillators with a linear distribution of individual frequencies for different α. The number of elements $N = 100$, $\omega_1 = 0.98$, $\Delta = 0.0001$.

where the phases ϕ_j are introduced via (23). Then Eq. (55) can be rewritten as:

$$\begin{aligned} \dot{x}_j &= -\omega_j y_j - z_j - \omega_j \alpha(\sin(\phi_{j+1} - \phi_j) + \sin(\phi_{j-1} - \phi_j))y_j, \\ \dot{y}_j &= \omega_j x_j + a y_j + \omega_j \alpha(\sin(\phi_{j+1} - \phi_j) + \sin(\phi_{j-1} - \phi_j))x_j, \\ \dot{z}_j &= b - c z_j + x_j z_j, \qquad j = 1, \ldots, N. \end{aligned} \tag{57}$$

The dependencies of the mean frequencies Ω_j on the parameter α with linear (Fig. 14), respectively random (Fig. 15) distributions of the individual frequencies exhibit the onset of PS for a small coupling term. The critical value α^* of a chain of Rössler oscillators is greater than the one for two Rössler oscillators, already hinted by Eq. (53).

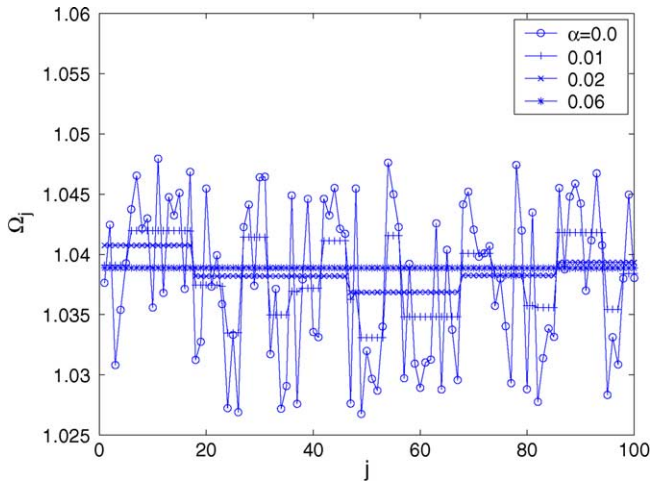

Fig. 15. Mean frequencies Ω_j in a chain of Rössler oscillators with randomly distributed frequencies in the interval [0.98,1] for different α. The number of elements $N = 100$.

11. Synchronization of globally coupled chaotic oscillators

Finally we study the potential of the presented method for *globally* coupled Rössler oscillators:

$$\begin{aligned}
\dot{x}_j &= -(\omega_j + \alpha_j u_j) y_j - z_j, \\
\dot{y}_j &= (\omega_j + \alpha_j u_j) x_j + a y_j, \\
\dot{z}_j &= b - c z_j + x_j z_j, \\
\dot{u}_j &= -\gamma_j u_j + x_j \textstyle\sum_{k=1,k\neq j}^{N} \beta_k y_k, \qquad j = 1, \ldots, N.
\end{aligned} \tag{58}$$

We take the same parameters of individual elements as in the previous section and randomly distributed frequencies ω_j. Let us choose again all $\gamma_j \gg 1$. Then the filtered control variable u_j can be described in the form:

$$u_j = \sum_{k=1,k\neq j}^{N} \sin(\phi_j - \phi_k), \tag{59}$$

and (58) can be rewritten as:

$$\begin{aligned}
\dot{x}_j &= -\omega_j y_j - z_j - \omega_j \alpha \textstyle\sum_{k=1,k\neq j}^{N} \sin(\phi_j - \phi_k) y_j, \\
\dot{y}_j &= \omega_j x_j + a y_j + \omega_j \alpha \textstyle\sum_{k=1,k\neq j}^{N} \sin(\phi_j - \phi_k) x_j, \\
\dot{z}_j &= b - c z_j + x_j z_j, \qquad j = 1, \ldots, N.
\end{aligned} \tag{60}$$

Following [23], we characterize the degree of synchronization by means of the *order parameter*:

$$R = \lim_{N\to\infty} \frac{N_l}{N}, \tag{61}$$

where N_l is the size of the largest cluster of synchronized oscillators. This frequency order parameter is for fully incoherent oscillators $R = 0$, and reaches for globally synchronized behavior the maximum $R = 1$. The order parameter R averaged over 10 samples of randomly distributed frequencies ω_j is presented in Fig. 16. We see that there

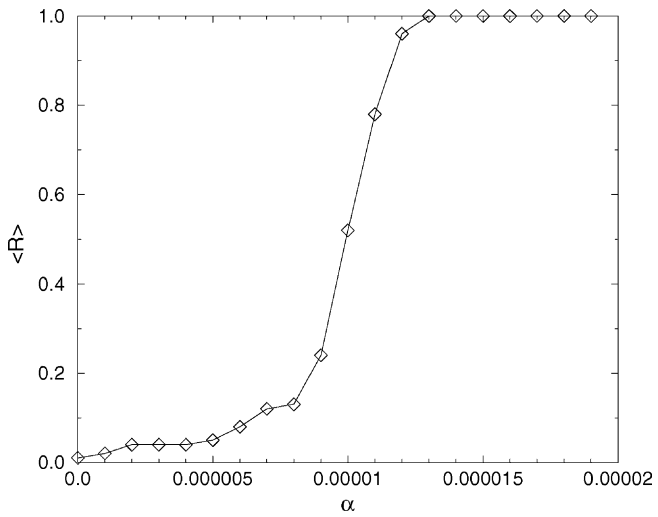

Fig. 16. Frequency entrainment in the ensemble of globally feedback coupled Rössler oscillators with randomly distributed frequencies in the interval [0.98,1] vs. α. The number of elements is $N = 100$.

exists a critical value α^* when all oscillators become synchronized. This transition from a fully incoherent behavior to a fully coherent (synchronized one) has been typically observed in ensembles of globally coupled elements.

12. Other forms of this control mechanism

It is important to emphasize that this principle can be applied not only to coupled self-oscillatory systems. For example, let us consider a simple controlled linear oscillator:

$$\begin{aligned} &\dot{x} = y, \\ &\dot{y} = (\omega^2 + \alpha u)x + \lambda y, \\ &\tau\dot{u} = -u + \beta xy. \end{aligned} \tag{62}$$

As a result of the control ($\alpha \neq 0$ in (62)), a stable limit cycle appears. So the balance of phase and amplitude is achieved by the same mechanisms of frequency control as in (2). Note, that at $\tau = 0$, i.e. $u = \beta xy$, the system (62) becomes the classical van der Pol equation related to a natural self-excited generator. This observation may be interpreted as *self-control* leading to a synchronization of voltage (x) and current (y) in the generator circuit.

Another control principle very similar to Eq. (2) can be used for system (1), when the variable $x_1(x_2)$ increasing (decreasing) with some characteristic exponent $\omega_1(\omega_2)$ for some bounded interval. Then, the system (1) describes a *growth-decay* process. In order to manage this process we apply the same type of feedback control, i.e. we use the quadratic form, but, here we add our control variable u directly to the process velocities:

$$\begin{aligned} &\dot{x}_{1,2} = F_{1,2}(x_{1,2}, \omega_{1,2}) + \alpha_{1,2}u, \\ &Lu = Q(x_1, x_2), \end{aligned} \tag{63}$$

where we state that some chosen (L, Q)-pair in Eq. (63) leads to the emergence of balanced (synchronized) oscillations of x_1 and x_2. As an example let us consider a *"predator–prey" system* [26]:

$$\begin{aligned} &\dot{x}_1 = \omega_1 x_1(1 - x_1) + \alpha_1 u, \\ &\dot{x}_2 = -\omega_2 x_2 + \alpha_2 u, \\ &\tau\dot{u} = -u + \beta x_1 x_2. \end{aligned} \tag{64}$$

This system has a globally stable limit cycle, i.e. variables x_1 and x_2 become balanced. For $\tau = 0$ the system (64) is the Lotka–Volterra-type equation from mathematical ecology. They demonstrate the role of a hidden self-control interaction $\beta x_1 x_2$, causing the self-organization between predator's growth and prey's decay.

In the proposed control schemes the control in the form of some quadratic form is applied multiplicatively in order to achieve the PS and additively in order to achieve the growth-decay rates balance.

13. Conclusions

In this paper we have presented a novel feedback control method for automatic phase locking of regular and chaotic oscillators. The main advantages of this method compared to more conventional schemes are the following:

- *The effect of the amplitudes* of the interacting subsystems on the difference of their phases provides a high efficiency of this approach: large amplitudes lead to a small phase difference.
- The proposed method can be used for automatic synchronization of oscillators of different nature (regular and chaotic), and different topology (e.g. coupled Rössler and Lorenz oscillators) and complexity (e.g. chaotic and hyper-chaotic Rössler oscillators).

- Phase synchronization already sets in at very small values of control parameters, which is very important from an energetical point of view. On the other hand, for specific parameter values synchronization cannot be obtained at all, that seems to be a trade-off.
- The method can be used to synchronize elements coupled in small (two units) and large (chains and lattices) ensembles. In the latter case the coupling can be local or global.

This presented approach can be helpful (i) for the understanding of self-organization mechanisms in many systems in nature and (ii) for the design of different schemes of automatic synchronization and could be applied to communication, engineering, ecology, and medicine.

Acknowledgements

We thank A. Pikovsky and M. Rosenblum for useful discussions. VNB acknowledges financial support from INTAS (Project No. 01-2061), SFB 555 and RFBR (Project No. 02-01-00968). GVO acknowledges financial support from RFBR (Project No. 03-02-17543 and 02-02-17573) and DAAD. NK and BB acknowledge the Volkswagen Stiftung. JK acknowledges SFB 555 and EU RTN (Contract No. HPRN-CT-2000-00158).

References

[1] A.S. Pikovsky, M.G. Rosenblum, J. Kurths, Synchronization – A Universal Concept in Nonlinear Sciences, Cambridge University Press, Cambridge, 2001.
[2] R.C. Elson, et al., Phys. Rev. Lett. 81 (1998) 5692;
C. Schäfer, et al., Nature 392 (1998) 239;
P. Tass, et al., Phys. Rev. Lett. 81 (1998) 3291;
V. Belykh, I. Belykh, M. Hasler, Phys. Rev. E 62 (2000) 6332;
A. Neimann, X. Pei, D.F. Russell, W. Wojtenek, L. Wilkens, F. Moss, H.A. Braun, M.T. Huber, K. Voigt, Phys. Rev. Lett. 82 (1999) 660.
[3] B. Blasius, A. Huppert, L. Stone, Nature 399 (1999) 354.
[4] L. Fabiny, P. Colet, R. Roy, Phys. Rev. A 47 (1993) 4287;
R. Roy, K.S. Thornburg Jr., Phys. Rev. Lett. 72 (1994) 2009;
V.S. Anishchenko, et al., Int. J. Bifur. Chaos Appl. Sci. Eng. 2 (1992) 633;
D. DeShazer, et al., Phys. Rev. Lett. 87 (2001) 044101;
V. Belykh, I. Belykh, E. Mosekilde, Phys. Rev. E 63 (2001) 036216;
E. Rosa, E. Ott, M.H. Hess, Phys. Rev. Lett. 80 (1998) 1642.
[5] J. Kurths (Ed.), A special issue on phase synchronization in chaotic systems, Int. J. Bifur. Chaos 11 (2000);
S. Boccaletti, et al., Phys. Rep. 366 (2002) 1.
[6] L.M. Pecora, T.L. Carroll, Phys. Rev. Lett. 64 (1990) 821;
H. Dedieu, M.P. Kennedy, M. Hasler, IEEE Trans. Circuits Syst.: Part II 40 (1993) 634;
L. Kocarev, U. Parlitz, Phys. Rev. Lett. 74 (1995) 5028.
[7] B. van der Pol, Phil. Mag. 43 6 ser. (1922) 700.
[8] M. Rabinovich, et al., Phys. Rev. Lett. 87 (2001) 068102.
[9] H. Haken, J.A.S. Kelso, H. Bunz, Biol. Cybern. 51 (1985) 347.
[10] J.D. Murray, Mathematical Biology, Springer, Berlin, 1989.
[11] A.H. Cohen, P.J. Holmes, R.H. Rand, J. Math. Biol. 13 (1982) 345.
[12] K. Wiesenfeld, et al., Phys. Rev. Lett. 65 (1990) 1749.
[13] W.C. Lindsey, Synchronization Systems in Communication and Control, Prentice-Hall, Englewood Cliffs, NJ, 1972.
[14] E. Ott, C. Grebogi, J.A. Yorke, Phys. Rev. Lett. 64 (1990) 1196;
K. Pyragas, Phys. Lett. A 170 (1992) 421;
for a review of control techniques and algorithms see S. Boccaletti, et al., Phys. Rep. 329 (2000) 103.
[15] N.J. Mehta, R.M. Hendersen, Phys. Rev. A 44 (1991) 4861;
Y.C. Lai, C. Grebogi, Phys. Rev. E 47 (1993) 2357;
T.C. Newell, et al., Phys. Rev. E 49 (1994) 313;

R. Konnur, Phys. Rev. Lett. 77 (1996) 2937;
M.-Ch. Ho, Y.-Ch. Hung, Ch.-H. Chou, Phys. Lett. A 296 (2002) 43.
[16] A. Pogromsky, H. Nijmeijer, IEEE Trans. Circuit Syst.: Part I 48 (2001) 152;
A.Yu. Pogromsky, G. Santoboni, H. Nijmeijer, Physica D 172 (2002) 65.
[17] Often, the time dependence rates (or frequencies) can be expressed in terms of multipliers of the right hand parts: $\dot{x}_{1,2} = \omega_{1,2} F_{1,2}(x_{1,2})$.
[18] Y. Aizawa, Prog. Theor. Phys. 56 (1976) 703.
[19] D. Christiansen, P. Alstrom, M.T. Levinsen, Physica D 56 (1992) 23.
[20] R. Eckhorn, et al., Biol. Cybern. 60 (1987) 121.
[21] J. Guckenheimer, P. Holmes, Nonlinear Oscillations, Dynamical Systems and Bifurcations of Vector Fields, Springer, Berlin, 1990.
[22] H. Haken, Synergetics: An Introduction, Springer, Berlin, 1977.
[23] Y. Kuramoto, Chemical Oscillations, Waves and Turbulence, Springer, Berlin, 1984.
[24] P. Tass, H. Haken, Z. Phys. B 100 (1996) 303.
[25] D.G. Aronson, G.B. Ermentrout, N. Kopell, Physica D 41 (1990) 403.
[26] A. Kolmogorov, G. Inst. Ital. Attuari 7 (1936) 74.
[27] C. Sparrow, The Lorenz Equations: Bifurcations, Chaos and Strange Attractors, Springer-Verlag, Berlin, 1982.
[28] O.E. Rössler, Phys. Lett. A 57 (1976) 397.
[29] For $\omega_1 = 1$ in the chaotic Rössler oscillator the mean in the time frequency does not equal to 1 and therefore, uncoupled oscillators have some frequency mismatch.
[30] E.F. Stone, Phys. Lett. A 163 (1992) 367.
[31] A.S. Pikovsky, M.G. Rosenblum, G.V. Osipov, J. Kurths, Physica D 104 (1997) 219.
[32] G.V. Osipov, B. Hu, Ch. Zhou, M. Ivanchenko, J. Kurths, Phys. Rev. Lett. 91 (2003) 24101.
[33] M. Rosenblum, A. Pikovsky, J. Kurths, Phys. Rev. Lett. 76 (1996) 1804.
[34] M.L. Rosenzweig, Science 171 (1971) 385.
[35] B. Blasius, L. Stone, Int. J. Bifur. Chaos 10 (2000) 2361.
[36] B. Blasius, E. Montbrio, J. Kurths, Phys. Rev. E 67 (2003) 035204R;
E. Montbrio, B. Blasius, Chaos 13 (2003) 291.
[37] V.S. Afraimovich, V.I. Nekorkin, G.V. Osipov, V.D. Shalfeev, Stability, Structures and Chaos in Nonlinear Synchronization Networks, World Scientific, Singapore, 1994.